Available online at www.sciencedirect.com
SCIENCE DIRECT
Journal of Power Sources 155 (2006) 213–218
JOURNAL OF POWER SOURCES
www.elsevier.com/locate/jpowsour

Measurements of humidity and current distribution in a PEFC

H. Nishikawa [a,*], R. Kurihara [a], S. Sukemori [a], T. Sugawara [a], H. Kobayasi, S. Abe [a], T. Aoki [b], Y. Ogami [b], A. Matsunaga [b]

[a] *Department of Electrical Engineering Tokyo Denki University, 2-2 Kandanishiki-cho, Chiyoda-ku, Tokyo 101-8457, Japan*
[b] *Fuel Cell Technology Development Department Toshiba Fuel Cell System,4-1 Ukishima-cho, Kawasaki-ku, Kawasaki-shi, Kanagawa 210-0862, Japan*

Received 19 March 2005; accepted 21 April 2005
Available online 11 July 2005

Abstract

Voltage decreases of polymer electrolyte fuel cells (PEFC) are affected by the relative humidity of the reaction gas inside the cells. A study was conducted to establish a method for measuring relative humidity and current distribution inside PEFC cells in order to identify the factors affecting the voltage decay of such fuel cells. The humidity distribution was measured using a humidity sensor for directly monitoring the relative humidity of the reaction gas flowing through the air flow channel of the cathode separator. The current distribution was measured directly by attaching a current sensor to the rib of the cathode separator. Typical results of relative humidity and current distribution are described and interpretations are discussed.

Keywords: PEFC; Humidity distribution; Current distribution

1. Introduction

There is increasing interest in the development of polymer electrolyte fuel cells (PEFC) because their compact size, light weight and high efficiency makes them attractive for automobiles and residential use. High performance fuel cells have been developed by reducing the thickness of polymer membranes [1] and improving the activity of catalysts [2]. However, there are still demands for a cell lifetime longer than the current one of only 20,000 h, that is, only half of the desired longevity of 40,000 h [3]. Cell voltage is known to deteriorate due to flooding under conditions of excess humidity [4,5], membrane degradation due to low humidity [6], increases of cell resistance due to incorporation of ionic contaminants [7] and repetitive load changes [8]. To simplify the system and increase efficiency it is desirable to reduce humidity levels but as humidity is decreased the rate of cell voltage degradation increases and lifetime becomes even shorter.

In this paper, we report the results of a study carried out to establish a technology for measuring relative humidity and current distribution inside PEFC cells in order to identify the sources of voltage degradation of these fuel cells.

2. Measurement of relative humidity and current distribution

A new method was proposed for measuring the relative humidity and current distribution using cells having dimensions of 17 cm × 17 cm [9,10].

2.1. Measurement of relative humidity distribution

A method was developed for measuring the relative humidity of the reaction gas flowing through the air flow channel of the cathode separator using a humidity sensor. Fig. 1 shows the method used for measuring the humidity distribution inside the cell. A 1 mm diameter hole was opened in the air flow channel and a stainless steel pipe

* Corresponding author. Tel.: +81 3 5280 3692; fax: +81 3 5280 3687.
E-mail address: nishik@e.dendai.ac.jp (H. Nishikawa).

0378-7753/$ – see front matter © 2005 Elsevier B.V. All rights reserved.
doi:10.1016/j.jpowsour.2005.04.032

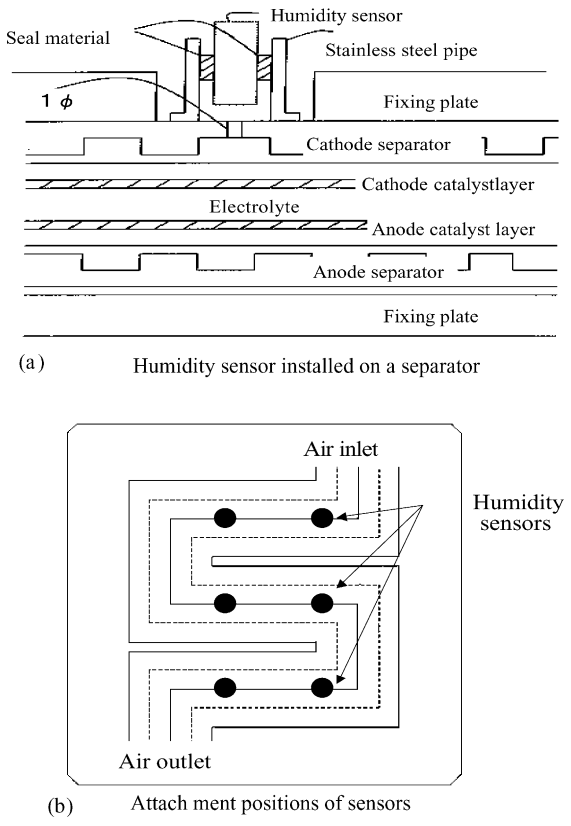

Fig. 1. Humidity distribution measurement. (a) Humidity sensor installed on a separator and (b) attachment positions of sensors.

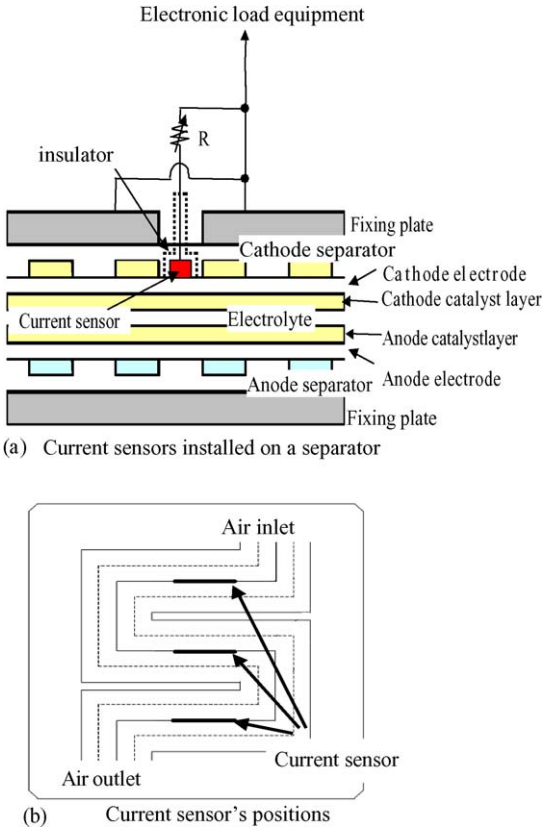

Fig. 2. Current distribution measurement. (a) Current sensors installed on a separator and (b) current sensor's positions.

attached and fixed to its circumference. The relative humidity of the reaction gas of the air flow channel was measured using this configuration. A commercially available Vaisala portable humidity–temperature meter HM141 and sensor HMP42 were used. The sensor diameter was 4 mm and its length was 23.5 cm. As shown in Fig. 1(b), measurements were made at six locations along the direction of the air flow.

2.2. Measurement of current distribution

The current distribution of cells is generally measured by dividing the cell, connecting shunt resistances to each section and making measurements [11–13]. We studied a measurement configuration where a current sensor is attached to a cell. The possibility of varying the size of the current sensor gives the advantage of allowing using this method for small size cells. Fig. 2 shows the current distribution measurement method developed in this study. The current sensor was inserted into the rib of the cathode separator and all areas except those connected to the MEA, were covered by insulation. The resistor was connected to the lead lines and the fixing plate. The current flowing through the lead wire was measured using a Tektro AM503B dc current probe. Fig. 2(b) shows the three locations where the current was measured.

The experiments were carried out using a cell having dimensions of 17 cm × 17 cm and a membrane thickness of 30 μm. Furthermore, in our experiments the humidity and current sensors were attached to separate cells and due to the sensor attachments the reaction area was approximately 260 cm^2.

3. Results of relative humidity and current distribution measurements

3.1. Relative humidity distribution results

An external humidifying method was used to vary the temperature of the humidifier and thereby regulate the humidity of the reaction gas flowing through the anode and cathode. The cell temperature was adjusted using a heater attached to the fixing plate. Since the humidity inside the cell is affected by the temperature of the measurement position, the humidity inside the cell and temperature of the measurement positions were measured simultaneously. The measured humidity results were corrected according to equation (1).

$$H = \text{measured relative humidity} \times \frac{P_1}{P_2} \quad (1)$$

where H is the corrected relative humidity (%), P_1 saturated vapor pressure at measurement temperature (Pa) ,and P_2: saturated vapor pressure at cell temperature (Pa).

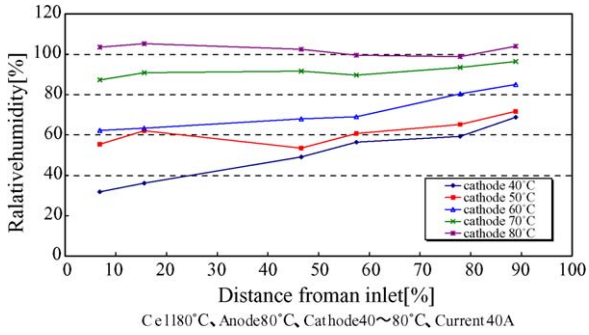

Fig. 3. Humidity distribution in a cell.

Fig. 3 shows the relative humidity on the cathode side when the cell temperature was 80 °C, the anode humidifying temperature 80 °C, the cathode humidifying temperature 40–80 °C and the current 40 A. When the cathode humidifying temperature was 40 °C, the relative humidity was 30% at the inlet of the cathode and gradually increased to 70% downstream of the air flow. Furthermore, the relative humidity inside the cell increased when the cathode humidity temperature was increased with the result that the distribution of the relative humidity inside the cell became more uniform.

In order to check the validity of this relative humidity distribution, we simulated relative humidity distribution using experimental data of the amount of water transported in a small size cell (5 cm × 5 cm) with almost the same membrane thickness. Measuring the amount of water transported involves monitoring the amount of water vapor that flows into and out of the anode and cathode [14,15]. The results from these experiments were used in combination with equations (2) and (3) to calculate the water transport coefficient per protons moving from the anode to the cathode.

$$\text{Cross A–C} = (\text{amount of water into the anode}) - (\text{amount of water out of the anode}) \quad (2)$$

$$\text{Cross C–A} = (\text{amount of water into the cathode}) + \text{product water} - (\text{amount of water out of the cathode}) \quad (3)$$

Here, Cross A–C is the amount of water transported from the anode to the cathode and Cross C–A is the amount of water transported from the cathode to the anode

$$\text{Water transport coefficient} = \frac{|\text{Cross C–A}| + |\text{Cross A–C}|}{2} \times \frac{96500}{18 \times I \times t} \quad (4)$$

Here, I is the current (A) and t is measurement time (s).

Fig. 4 shows the water transport measurement results obtained at a cell temperature of 80 °C, an anode humidifying temperature of 70 °C, a cathode humidifying temperature of 40–70 °C, with the current varying from 1–5 A,which corresponds to 40–200 mA cm^{-2}. Fig. 4(a) shows the amount

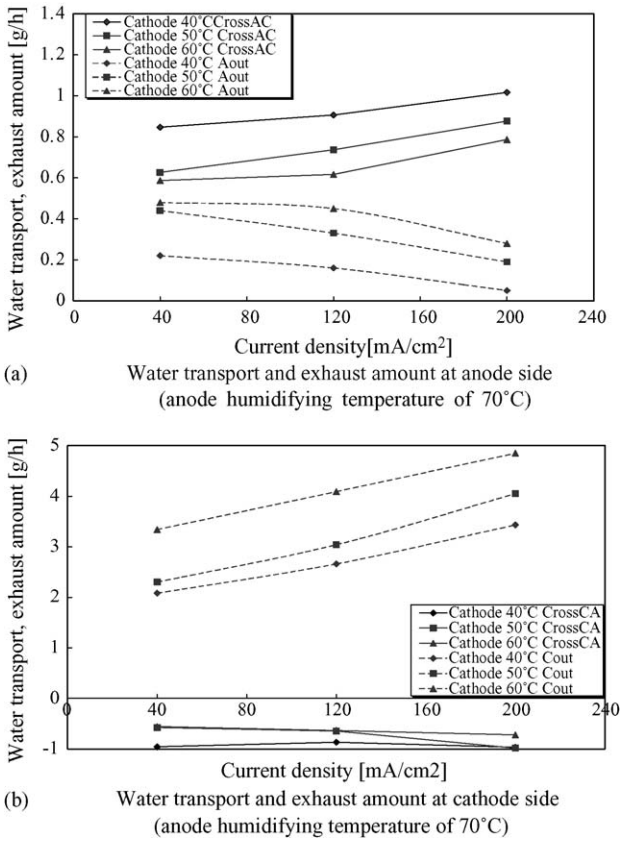

Fig. 4. Water transport and exhaust amount at: (a) anode side (anode humidifying temperature of 70 °C) and (b) cathode side (anode humidifying temperature of 70 °C).

of water transported from the anode to the cathode and the amount of water exhausted from the anode. Fig. 4(b) shows the amount of water transported from the cathode to the anode and the amount of water exhausted from the cathode. The water transport coefficient was calculated using these results. The water transport coefficient shows the amount of water transported per proton, where the amount of water transported from the anode to the cathode was determined by subtracting the back diffusion water from the electro-osmotic water.

Fig. 5(a) shows the water transport coefficient results. The water transport coefficient was found to decrease with increasing current and cathode humidifying temperature. The decrease of the water transport coefficient is thought to be due to the following sequence of events: (a) the current increase leads to an increased production of water; (b) the increase of the cathode humidity temperature is accompanied by an increase of the flow of water into the cathode; (c) this results in an increase of the water vapor pressure of the cathode and an increase of back diffusion water. Fig. 5(b) shows the same results at a humidifying temperature of 80 °C.

These results were used to simulate the relative humidity distribution. The relative humidity of the reaction gas in each segment was calculated by dividing the cells into ten sections and the current distribution and product water were assumed to be uniform in each of the divided segments.

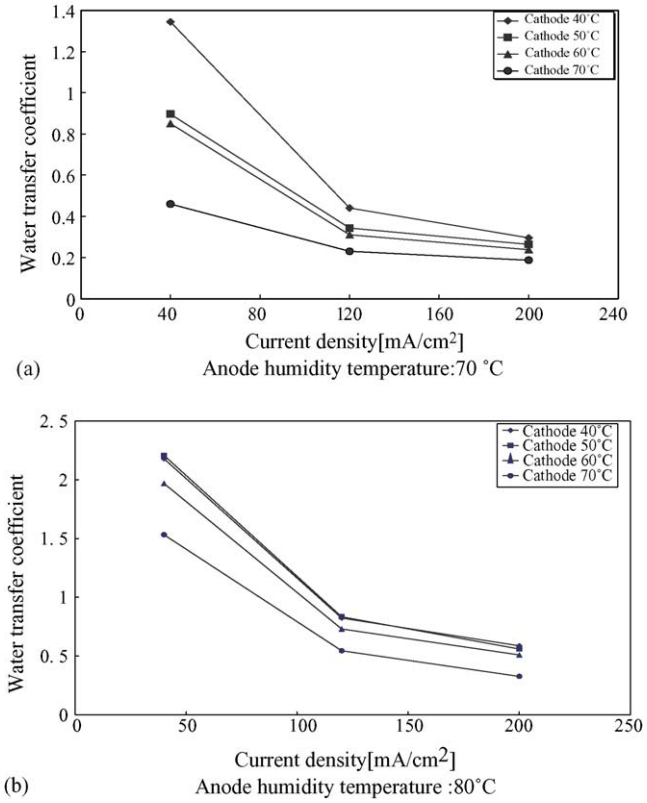

Fig. 5. Water transport coefficient. Anode humidity temperature: (a) 70 °C and (b) 80 °C.

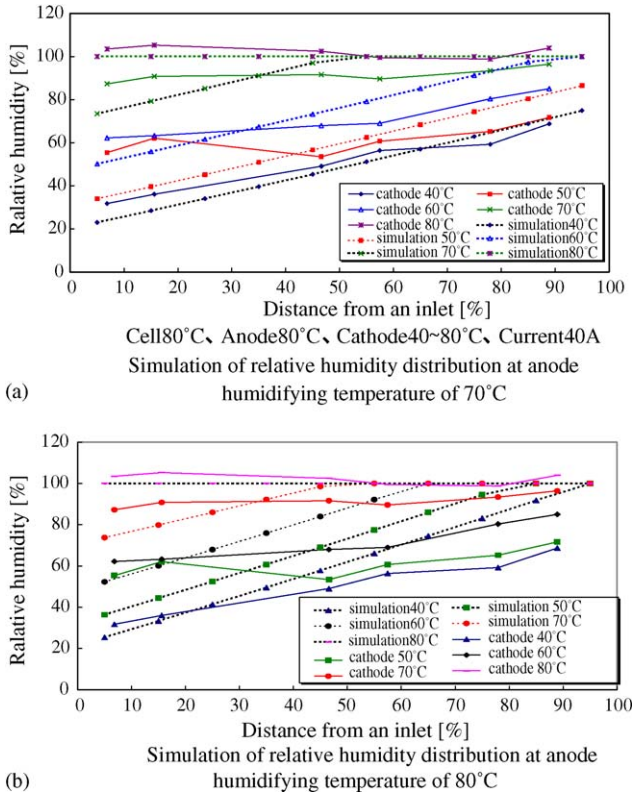

Fig. 6. Relative humidity distribution (comparison of measurement and simulation). Simulation of relative humidity distribution at anode humidifying temperature of (a) 70 °C and (b) 80 °C.

The water transported from the anode to the cathode was calculated using the water transport coefficients determined from experimental measurements. The relative humidity distribution results are shown in Fig. 6, where Fig. 6(a and b) shows the results for anode humidifying temperatures of 70 and 80 °C, respectively. Our simulation results are in good agreement with experimental values of the water transport coefficient obtained at an anode humidifying temperature of 70 °C. The water transport coefficient is affected by the back diffusion of water, that is, the load current, the humidifying temperature of the anode/cathode and flow pattern inside the cell. Thus, the flow pattern of the small size cell and of the 17 cm × 17 cm one are not necessarily identical. These factors may have some effects and we intend to investigate further the measurements of the water transport coefficient and the simulation method.

3.2. Current distribution results

Fig. 7 shows an example of the current distribution results where the air utilization was varied. In order to eliminate the changes of the current distribution due to differences of relative humidity inside the cell, the current distribution was measured at a cell temperature of 60 °C and an anode/cathode humidifying temperature of 60 °C. The air utilization was varied from 13% at 20 A.

The results showed that the up stream current increases when the air utilization surpasses 30%. The down stream current decreases and a change in the current distribution were observed. The magnitudes of the changes increase when the air utilization increased and when it was above 70%, a sudden drop of the central and down stream current was seen. This is thought to occur because the amount of water exhausting from the cell decreases when the air utilization is increased and as a result water remains inside the cell leading to flooding down stream of the cell.

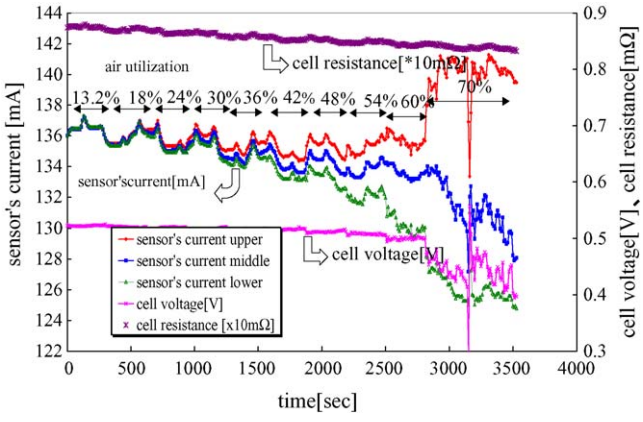

Fig. 7. Current distribution when in creasing air utilization.

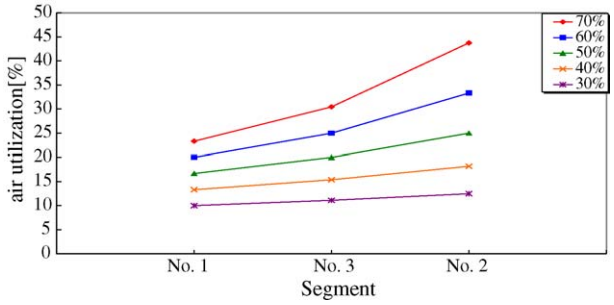

Fig. 8. Air utilization of each segment.

To better understand the experimental current distribution results we simulated the variation of current distribution with the air utilization.

The following procedure was used for the simulations: (1) the cell was divided into three sections; (2) the air utilization for each cell segment was calculated; (3) air utilization–cell voltage characteristics was obtained using a 5 cm × 5 cm cell; (4) the results were used to calculate the current distribution. Fig. 8 shows the air utilization of each individual segment when the air utilization was changed. Fig. 9 shows the experimental results for the air utilization characteristics obtained using the small size cell. Fig. 10 shows the calculated current distribution based on the results of Figs. 8 and 9 for the changes of air utilization. Current ratio of upstream and

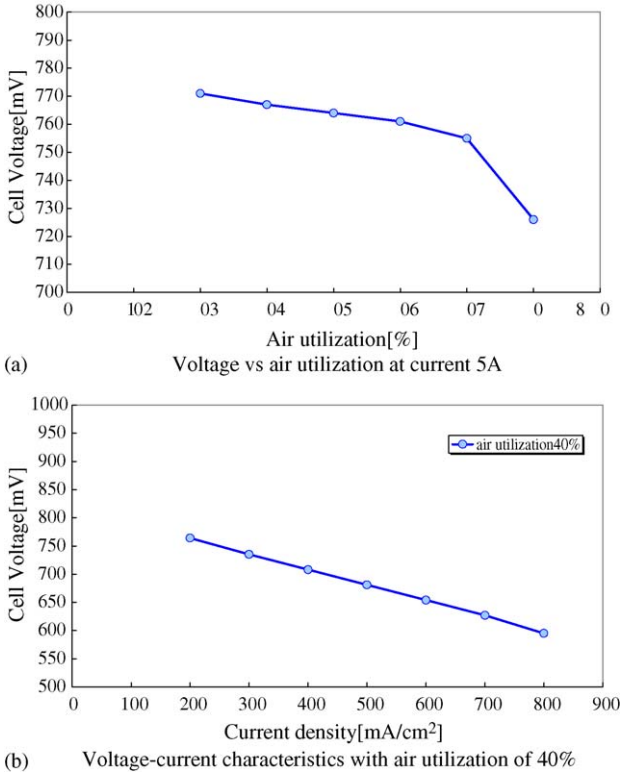

Fig. 9. Voltage–current characteristics with air utilization. (a) Voltage vs. air utilization at current 5 A and (b) voltage–current characteristics with air utilization of 40%.

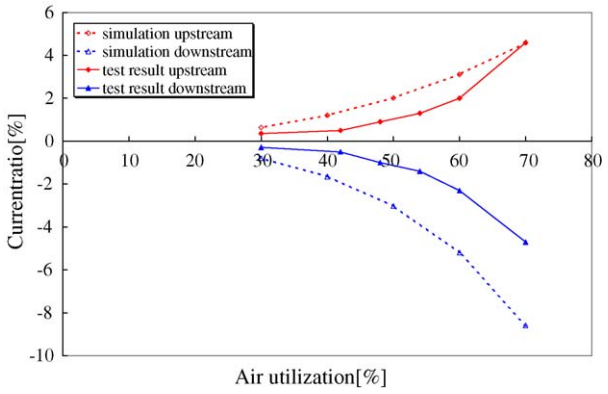

Fig. 10. Current distribution (comparison of measurement and simulation).

downstream in Fig. 10 means the ratio based on the central current. Both the experimental and simulated results show that increases of the air utilization are accompanied by increases of the changes of the current distribution. There is a reduction in the downstream current due to decreases of the concentration of downstream oxygen as a consequence of increases of the air utilization.

Fig. 11 shows current distribution results when the cathode reaction gas was changed from air to oxygen. In order to maintain the relative humidity inside the cell under the same conditions the flow of oxygen was kept the same as that of air. In Fig. 11, the values in parentheses shows the air utilization and the numbers below the parentheses, are the oxygen utilization. These results showed that when air was replaced by oxygen, then due to a reduction in the oxygen utilization: (a) the current distribution was almost negligible; (b) a small difference in the upstream and downstream current was observed when the oxygen utilization increased; (c) the onset of flooding for oxygen utilization became higher than 73%.

Fig. 12 shows the current distribution for a cell temperature of 80 °C and an anode humidifying temperature of 80 °C when the cathode humidifying temperature was slowly changed from 70 to 40 °C. When the cathode humidifying temperature was reduced then the upstream current was observed to decrease and the downstream current to increase.

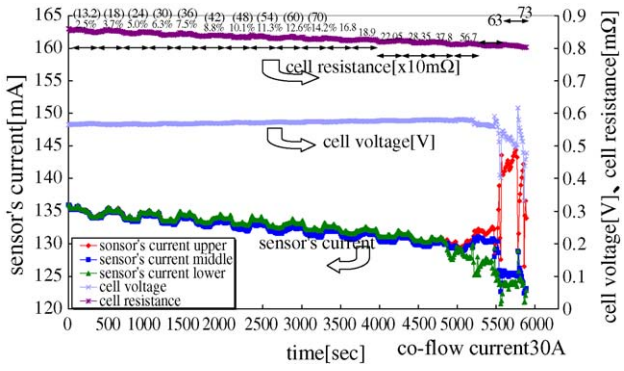

Fig. 11. Current distribution when increasing oxygen utilization.

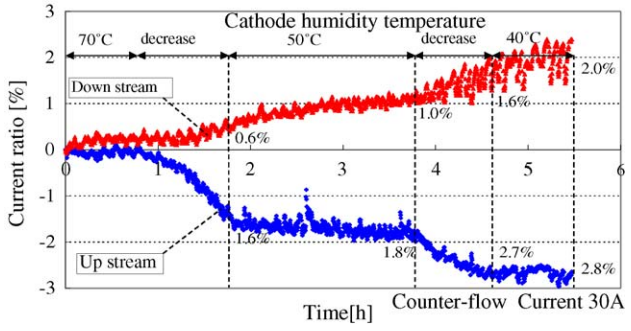

Fig. 12. Current distribution when decreasing cathode humidity temperature.

The reason for this can be seen from Fig. 3 where the relative humidity distribution shows that during low humidity operation, the relative humidity at the air inlet decreases and the relative humidity gradually increases in the downstream direction. That is, since the relative humidity of the upstream cathode is low, then the water content of the polymer membrane decreases. This not only leads to an increase of the resistance of the membrane but also to a decrease of the water content inside the ionomer of the catalytic layer. Consequently, proton conductivity and oxygen transport are adversely affected with the result that oxygen reduction reaction is reduced. Thus, the up stream current decreases due to the reduction of the catalyst utilization rate. However, since the downstream relative humidity increases, it is thought that the current also increased.

4. Summary

New methods for measuring the relative humidity distribution and current distribution inside PEFC cells were established. The measurements showed that

(1) The relative humidity of the air inlet was extremely small at 30%, at a cell temperature of 80 °C an anode humidifying temperature of 80 °C, and cathode humidifying temperature of 40 °C. Near the outlet the relative humidity reached 70% thus showing the existence of a large change between the relative humidity of the inlet and outlets.
(2) From current distribution measurements, it was found that with an increasing air utilization the upstream current increased and the downstream current decreased. However, when the cathode humidifying temperature was slowly reduced, then the upstream current decreased and the downstream current increased. The former observation of the decrease of the downstream current was related to an oxygen concentration dependence phenomena and the latter results due to phenomena related to cell resistance and catalyst utilization rate when operating at a low humidity temperature.

A technology for measuring relative humidity and current distributions is thus almost fully developed. In the future, these results will be used to study the factors affecting the degradation of the cell voltage.

Acknowledgement

This work was supported by the New Energy and Industrial Technology Development Organization (NEDO).

References

[1] A. Gasteiger, W. Gu, R. Makharia, M.F. Mathias, B. Sompalli, Beginning-of-life MEA performance-efficiency loss contribution, in: Handbook of Fuel Cells, vol. 3, Wiley, 2003, pp. 593–610 (Chapter 46).
[2] T.R. Ralph, G.A. Hards, J.K. Keating, Low cost electrodes for proton exchange membrane fuel cell, J. Electrochem. Soc. 144 (November (11)) (1997) 3845–3856.
[3] Y. Oomori, O. Yamazaki, T. Tabata, Evaluation study of PEFC using single cell at Osaka gas, in: The 11th FCDIC Symposium, 2004, pp. 99–102.
[4] J. St-Pierre, D.P. Wilkinson, S. Knights, M.L. Bos, Relation between water management, contamination and lifetime degradation in PEFC, J. Mater. Electrochem. Syst. 3 (2000) 99–106.
[5] S.D. Knights, K.M. Colbow, J.S. Pierre, D.P. Wilkinson, Aging mechanisms and lifetime of PEFC and DMFC, J. Power Sources 127 (2004) 127–134.
[6] Chengde Huang, Kim Seng Tan, Jianyi Lin, Kuang Lee Tan, XRD and XPS analysis of the degradation of the polymer electrolyte in H_2O_2 fuel cell, Chem. Phys. Lett. 371 (2003) 80–85.
[7] T. Okada, Effect of ionic contaminants, in: Handbook of Fuel Cells, vol. 3, Wiley, 2003, pp. 627–646 (Chapter 48).
[8] D.P. Wilkinson, J. St-Pierre, Durability, in: Handbook of Fuel Cells, vol. 3, Wiley, 2003, pp. 611–626 (Chapter 47).
[9] H. Nishikawa, R. Kurihara, S. Sukemori, M. Ando, M. Sato, Y. Ogami, A. Matsunaga, Measurement for humidity and current distribution in a PEFC cell, in: The 11th FCDIC Symposium, 2004, pp. 103–106.
[10] H. Nishikawa, R. Kurihara, S. Sukemori, T. Sugawara, H. Kobayashi, Y. Ogami, A. Matsunaga, Measurement for humidity and current distribution in PEFC cell, in: Fuel Cell Seminar, Poster Session 1, 2004.
[11] T. Suzuki, H. Yamada, Y. Morimoto, Measurement of the distribution of current density and ionic conductivity of a PEFC, in: The Ninth FCDIC Symposium, 2002, pp. 35–38.
[12] G. Bender, M.S. Wilson, T.A. Zawodzinski, Further refinements in the segmented cell approach to diagnosing performance in polymer electrolyte fuel cell, J. Power Sources 123 (2003) 163–171.
[13] E. Gulzow, S. Schonbauer, Tools for the Investigation of current densities in fuel cell, in: FC Seminar, 2003, pp. 252–255.
[14] W.-K. Lee, S. Shimpalee, J.W. Van Zee, Verifying prediction of water and current distribution in a serpentine flow field polymer electrolyte membrane fuel cell, J. Electrochem. Soc. 150 (3) (2003) A341–A348.
[15] M. Mizuhata, K. Oguro, H. Takenaka, Water transport phenomena in polymer electrolyte during operation of polymer electrolyte fuel cells, in: Proceedings of First Scientific Workshop for Electrochemical Materials, 1996, pp. 169–178.